A 3D Finite-Difference Analysis of Interaction between a Newly-Driven Large Tunnel with Twin Tunnels in Urban Areas

S. Akbari[1], Sh. Zare[1], H. Chakeri[2] and H. Mirzaei[2]

1-Shahrood University of Technology, Faculty of Mining, Geophysics and Petroleum Engineering, Shahrood, Iran
2-Sahand University of Technology, Dept. of Mining Engineering, Tebriz, Iran

Keywords	Abstract
	Evaluation of the interaction between a new and the existing underground structures is one of the important problems in urban tunneling. In this work, using FLAC3D, four numerical models of single- and twin-tube tunnels in urban areas are developed, where the horizontal distance between the single- and twin-tube tunnels are varied. The aim is to analyze the effects of the horizontal distances, considering various criteria such as the deformation of linings, the forces and moments exerted on the twin-tube tunnels and their safety factors, the subsidence that occur on the surface and the nearby buildings, the stability of the single-tube tunnel, and the stability of the pillar lying between the single- and twin-tube tunnels. Considering the above-mentioned criteria, the results obtained indicate that the interaction between the single- and twin-tube tunnels is virtually negligible in the distance more than three times the single-tube tunnel diameter. Also the stability of the pillar lying between the tunnels makes the distance to be chosen at least 1.5 times the single-tube tunnel diameter.

1. Introduction

The need for tunnels in urban areas due to urbanization and population has increased. Especially for the public transportation purposes, they have increased remarkably in the recent years [1]. In some cities, the geotechnical and underground conditions mean that new tunnels must be constructed close to the existing ones. When a new tunnel is bored close to an existing one, this may lead to important interaction effects. For example, the new tunnel construction may lead to unacceptable distortions or bending moments in the existing tunnel liner. The nature of these interactions depends significantly on the tunnel spacing, size of both tunnels, liner stiffness, and method used to excavate the tunnel. Therefore, it is of prime importance to predict the possible interaction between the structures during the design stage in order to maintain a stable tunneling operation.

The interaction between closely-spaced tunnels has been studied in the past using a variety of approaches including field observation, physical modeling, and numerical modeling [2-13].

Addenbrooke and Potts [8] have made 2D finite element analyses of multiple tunnels using a non-linear elastic perfectly plastic soil model. They concluded that for side-by-side tunnels, the interaction effects became negligible for a pillar width of > 7 diameter.

Hage and Shahrour [9] have shown that if the spacing between the tunnels is at least 3D, there is no significant effect. Most numerical modeling studies for the interaction between tunnels involve 2D analyses. However, 2D numerical analyses suffer from some major drawbacks, and a 2D model cannot be used to investigate the 3D interactions between tunnels.

Liu *et al*. [7] have investigated the effects of tunneling on the existing support systems in adjacent side-by-side, piggyback, and staggered parallel tunnels in the Sydney region using a full 3D finite element modeling. It was concluded that

the effects strongly depended on the relative locations of the existing and the new tunnels. In a region such as Sydney, with high horizontal regional stresses, driving a new tunnel in a piggyback position or staggered parallel to the existing tunnel more readily have caused adverse effects on the existing tunnel support system than a new side-by-side tunnel parallel to the existing tunnel.

Chakeri *et al*. [10] have conducted a study to investigate the interactions between tunnels. They observed that an increase in the horizontal spacing between twin tunnels resulted in a decrease in the settlement of the central part of the twin tunnels, and led to stabilization of the settlement above the tunnels.

Sarfaraz *et al*. [11] have investigated the interaction between two neighboring tunnels using PFC2D. In a study by Abdollahi *et al*. [12], using the numerical methods, an accurate simulation of the TBM motion has been carried out. They concluded that the tunnel was instable in the fault zone, and a combination of the umbrella arch and radial grouting methods were the most suitable strategies. In the study of Mirsalari *et al*. [13], the classical finite difference formulation (i.e. the backward, central, and forward finite difference formulations) has been hybridized using the boundary element formulation, enabling to obtain the nodal tangential stresses and horizontal strains along the elements.

In this work, we aimed to use a full 3D numerical technique, i.e. FLAC3D, to analyze the various important aspects of the interaction between the single- and twin-tube tunnels in a close proximity in Tabriz (Iran), while the large-diameter single-tube tunnel was being excavated at different horizontal distances from the already excavated relatively small-diameter twin-tube tunnels. The main objectives were as follow:

- Analyze the deformation pattern of the cross-sections of the twin-tube tunnels due to excavation of a large diameter single-tube tunnel with various horizontal distances;

- Study the forces and moments acting on the segmental linings of the twin-tube tunnels and their safety factors due to excavation of a large diameter single-tube tunnel with various horizontal distances;

- Investigate the surface subsidence occurring due to excavation of the twin and single-tube tunnels with various horizontal distances;

- Study the excavation stability of the single-tube tunnel in all the horizontal distances;

- Study the stability of the column lying between the twin- and single-tube tunnels in all the horizontal distances in order to obtain the distance in which all the interaction effects disappear and also the minimum allowable distance that could be reached without any extra stability charges.

2. Site Location and Geology

The twin-tube tunnels (Line 1) have been constructed under the Mohagegi Avenue, and the single-tube tunnel (Line 2) will be constructed close to the twin-tube tunnels in the same location. Figure 1 presents the location and cross-sections of the proposed tunnels. The twin-tube tunnels have a circular shape with a diameter of 6.88 m (Figure 1b). The single-tube tunnel also has a circular shape with a diameter of 9.5 m (Figure 1c).

According to the proposed plan, the mid-point of the twin- and single-tube tunnels was 20.52 m below the surface (Figure 2).

An extensive site investigation was carried out to determine the ground conditions. The characteristics of the four layers shown in Figure 2 are detailed in Table 1. Table 2 summarizes the mechanical properties of soil layers in which the tunnels are laid, considering the Poisson's ratio as 0.3.

Table 1. Characteristics of the geological layers around the tunnels.

Parameter	Layer 1	Layer 2	Layer 3	Layer 4
Ground type	Remolded soil	Upper silt	Silty sand	Lower silt
Thickness (m)	9	11.52	10	Undefined
Density (g/cm^3)	1.5	1.7	1.9	1.7
Elasticity modulus (MPa)	40	15	50	35
Internal friction angle (degree)	25	25	35	28
Cohesion (kPa)	5	20	5	25

Table 2. Mechanical properties of the soil layers around the tunnels.

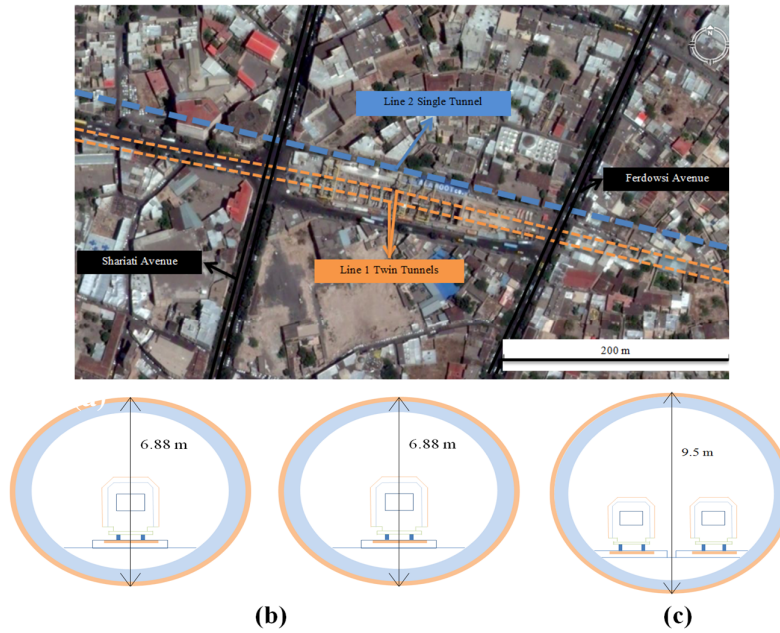| Parameter	Layer 1	Layer 2	Layer 3	Layer 4
Ground type	Remolded soil	Upper silt	Silty sand	Lower silt
Bulk modulus	33.33×10^6	12.5×10^6	41.66×10^6	29.16×10^6
Shear modulus	15.38×10^6	5.76×10^6	19.23×10^6	13.46×10^6

Figure 1. a) Location of tunnels b) Cross-section of the Line 1 twin-tube tunnels c) Cross-section of the single-tube tunnel.
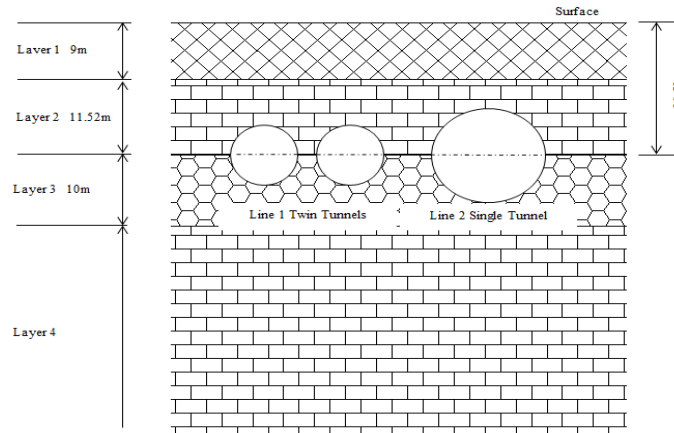

Figure 2. Lithology around the tunnels.

3. Modeling and numerical simulation procedure

Different numerical methods, for example, finite element, finite difference, boundary element, discrete element, and hybrid methods have been widely used for modeling underground excavations. In this work, FLAC3D (Fast Lagrange Analysis of Continua in 3-dimensions), which is based on the finite difference method, was used for modeling.

Since in this work, we aimed to evaluate the interaction effects in various horizontal distances of the single-tube tunnel and Sahand tunnel, considering various underlying criteria, four finite difference models with various horizontal distances of the single-tube tunnel and Sahand tunnel were generated. In Figure 3, the horizontal

distance (L) is given as the amounts of 1.5, 2, 2.5, and $3D_2$, where D_2 is the single-tube tunnel's diameter.

Horizontal distance between Line 1 twin tunnels and Line 2 single tunnel ($1.5D_2$, $2D_2$, $2.5D_2$, $3D_2$)
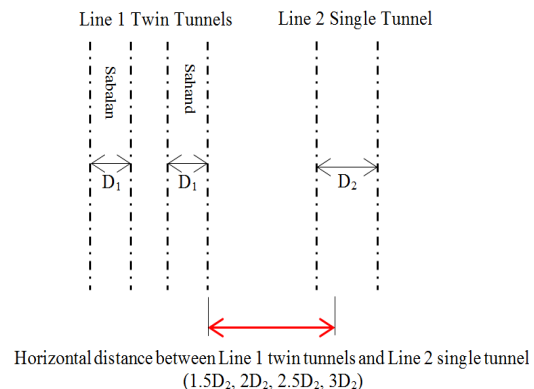
Figure 3. Plan of the twin- and single-tube tunnels.

Several parametric studies have been carried out in the previous work to evaluate the minimum dimensions of the domain size. As a result, the following values were obtained [14]:

- (H + 4D), for the mesh height,
- (H + 3D), for the mesh length,
- 3H, for the mesh width.

where H is the tunnel axis depth and D is the tunnel diameter.

In order to avert any impact from the boundaries, the sizes of all the four domains were selected as larger than the above-mentioned minimum allowable values, according to the depth (H) and diameter of the large diameter single-tube tunnel (D_2). Due to the changes that had to be made in the horizontal distance between the single and double tube tunnels (L), the widths of the generated models were different according to the position of the large diameter single-tube tunnel (Figure 4).
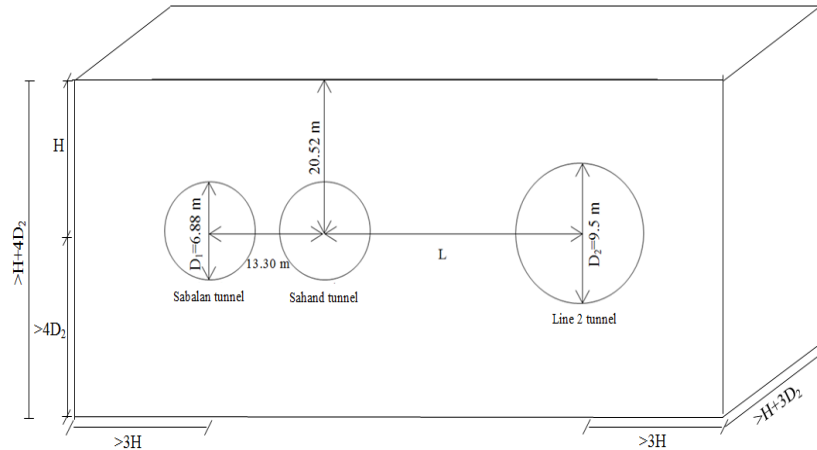

Figure 4. A 3D schematic view of the model.

Figure 5 shows the 3D isometric views of the generated models. Shell elements were used for modeling both the shield and the segmental linings. At the shell elements, each node comprises six degrees of freedom, namely three for displacements and three for rotations.
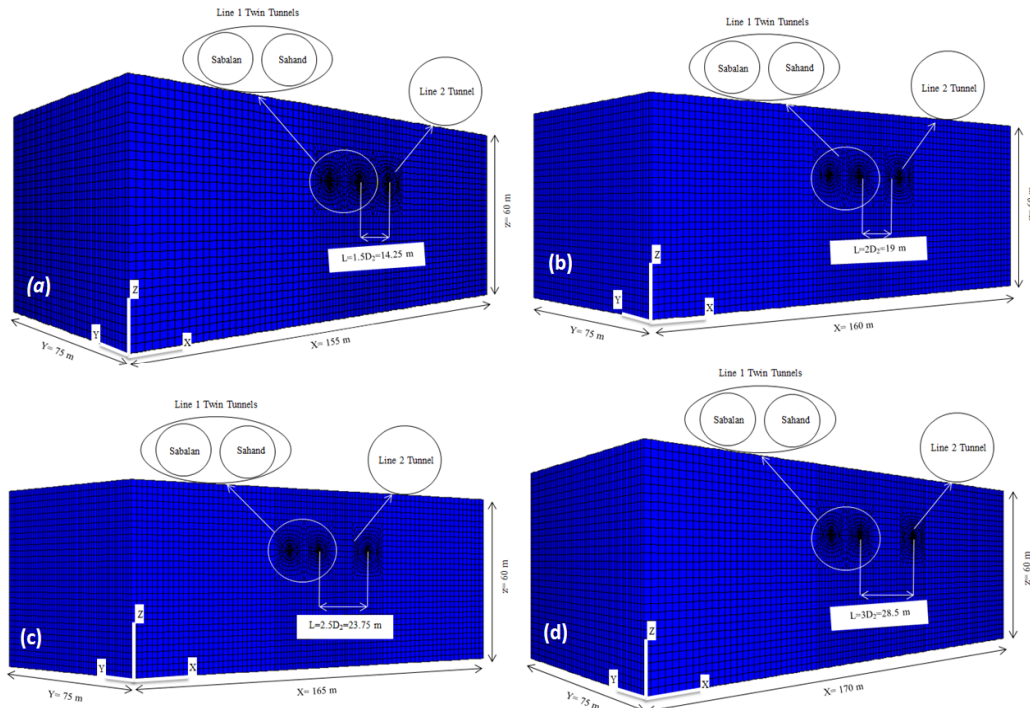

Figure 5. 3D isometric view of the model. *a*) L = 1.5D_2 b) L = 2D_2 c) L = 2.5D_2, d) L = 3D_2

The movements in the vertical direction were fixed at the bottom boundary of the mesh. No horizontal displacements were allowed on the x-z and y-z planes at the boundaries of the mesh. As a result of site investigations and with reference to the internal friction angle of soil layers in which the tunnels were laid (Table 1), the earth pressure at rest (i.e. $k_0 = 1 - \sin\varphi$) was taken as $k_0 = 0.5$. The live loads exerted on the surface were taken as 20 kN/m² for traffic and buildings.

The Mohr-Coulomb constitutive model was used to represent the soil layers. This model is the conventional model used to represent the shear failure in soils and rocks. Also the water table was taken as 9 m below the surface of the studied area. The tunnel excavation process was modeled using a step-by-step approach. In each step, the excavation length increment was taken as 1.5 m. Also a spacing of 9 m (for shield length) was taken between the tunnel face and the last embedded segmental lining for both the twin- and single-tube tunnels. First, the tunnel face was excavated by an EPB machine using the shell elements to simulate the shield, and then the tunnel was supported using the segmental linings and the precast grouting elements. According to the process that was used for excavation of the twin-tube tunnels and to reach a close correspondence between the simulation and the actual excavation process, the face and grouting pressures were taken as 1 and 2.5 bar, respectively. Based on the actual excavation sequence and spacing between the faces of the twin-tube tunnels, first, the Sahand tunnel was excavated for the full length of the model, and then the Sabalan tunnel and Line 2 single-tube tunnel were excavated using the above-mentioned construction process. The geometrical characteristics of the twin- and single-tube tunnels are presented in Tables 3 and 4, respectively.

Table 3. Geometrical characteristics of the twin-tube tunnels.

Geometrical parameter	Amount (m)
External diameter	6.88
Internal diameter	6
Segmental lining thickness	0.30
Grouting thickness	0.14
Spacing between tunnels	13.30

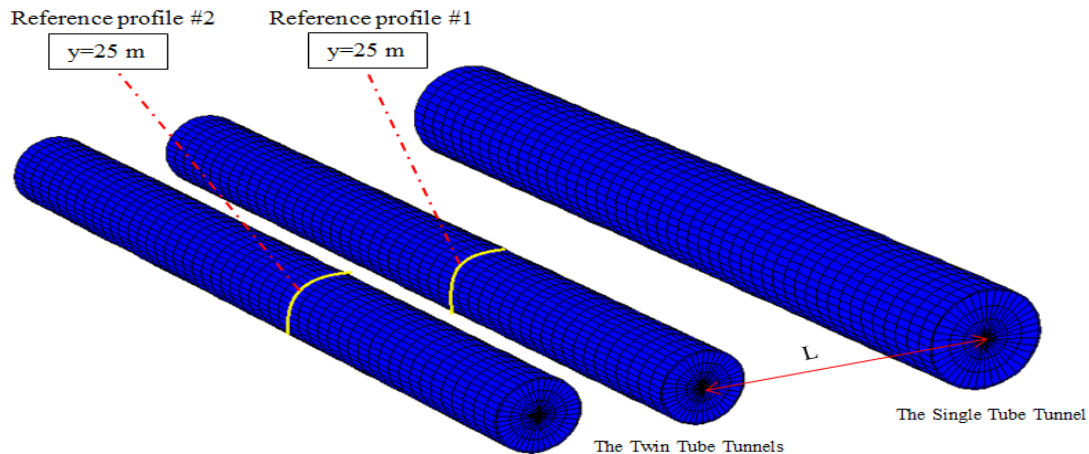**Table 4. Geometrical characteristics of the single-tube tunnel.**

Geometrical parameter	Amount (m)
External diameter	9.5
Internal diameter	8.5
Segmental lining thickness	0.35
Grouting thickness	0.15

4. Effects of tunneling on the existing support system

This section presents the results of the interaction behavior between the twin- and single-tube tunnels observed when the single-tube tunnel was excavated at various horizontal distances from the existing twin-tube tunnels.

4.1. Investigation of horizontal distances on deformation pattern

Two reference sections on the Line 1 twin-tube tunnels were selected for monitoring the deformation patterns related to the different horizontal distances of the Line 2 single-tube tunnel. Both sections were selected at the mid-point of the excavation length (y = 25 m) in order to avoid the boundary effects (Figure 6).

Figure 6. Isometric view of the tunnels together with the reference cross-sections at the twin-tube tunnels.

The deformed sections of the Sahand and Sabalan tunnels for different horizontal distances of the single-tube tunnel (L) are shown with a 50-fold exaggeration in Figure 7. (L = 1.5, 2, 2.5, and $3D_2$, where D_2 is the single-tube tunnel's diameter.)
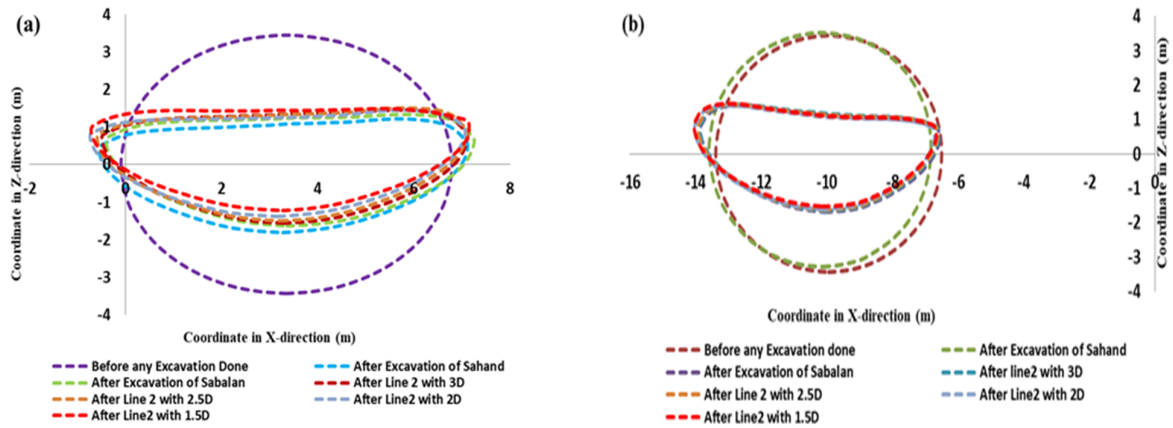

Figure 7. Deformation patterns of the sections of the twin tunnels based on the different horizontal distances. a) Sahand tunnel b) Sabalan tunnel.

As it can be seen, the distortion of the sections of both the Sahand and Sabalan tunnels is at its maximum level due to the excavation of the tunnel itself. Excavating the single-tube tunnel makes the sections of both twin-tube tunnels move slightly to the opposite-side and upward. It could also be seen that the amounts of deformations that occurred at the Sahand's section due to the excavations of Line 2 single-tube tunnel were higher than those at the Sabalan's section; this seems logical due to the lower interaction between the Line 2 and Sabalan tunnels.
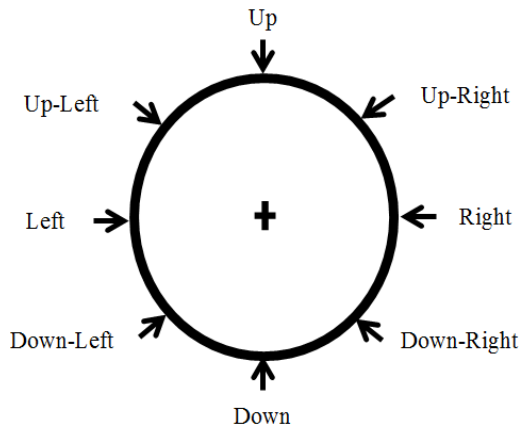
4.2. Effects of tunneling on internal forces of existing support system

During the modeling several points, as marked in Figure 8, are monitored to quantify the effects of tunneling on the existing support system. The forces and moments exerted on the segmental linings of the existing twin-tube tunnels due to excavation of the single-tube tunnel with various horizontal distances are presented in Table 5.

Table 5. Forces and moments exerted on the segmental linings of twin-tube tunnels with various horizontal positions of the single-tube tunnel.

Tunnel's name	Check-point position	1.5D			2D			2.5D			3D		
		N_x (KN)	M_x (KN.m)	Q_x (KN)	N_x (KN)	M_x (KN.m)	Q_x (KN)	N_x (KN)	M_x (KN.m)	Q_x (KN)	N_x (KN)	M_x (KN.m)	Q_x (KN)
Sahand	Up	651	5	2	620	2	8.5	610	3	11	600	5	6
	Up-right	840	17	15	780	8	15	760	4.4	15	745	3.41	2.5
	Right	1080	20.88	85	1030	13.24	68	1020	8.31	60	1015	4.32	72
	Down-right	960	5.2	50.8	934	4.2	41.4	915	4.2	34.4	900	5	50.9
	Down	740	21	0	717	18.87	0	698	16.17	2	682	12.97	3
	Down-left	894	6	30	876	4.6	28.7	866	4	26.6	850	4.5	39.1
	Left	1055	31.28	37	1030	31.63	36	1030	29.22	35	1025	26.27	32.5
	Up-left	874	12.5	10	857	16	6	840	16.5	6	840	16	6.74
Sabalan	Up	580	15	3	580	17	2.5	560	21	4	560	23	1
	Up-right	750	4.8	22	760	5.47	25	740	5.11	30	740	4.06	17.5
	Right	1000	3	52.1	1000	6	51.1	1000	10	52	1000	12	52
	Down-right	900	0.5	16.8	900	1.2	14.3	900	1.8	10	900	1.7	20
	Down	680	1	4.4	680	2	3	660	5	3	660	7	2
	Down-left	820	2.56	7	820	2	5	820	1.7	3	820	2.22	11
	Left	1000	3.5	35.4	1000	0.5	34	1020	2.5	33	1020	4	29
	Up-left	800	9.5	25	800	9.5	30	800	9	30	800	10	17.5

Figure 8. Points adopted on the segmental lining to monitor the forces and moments.
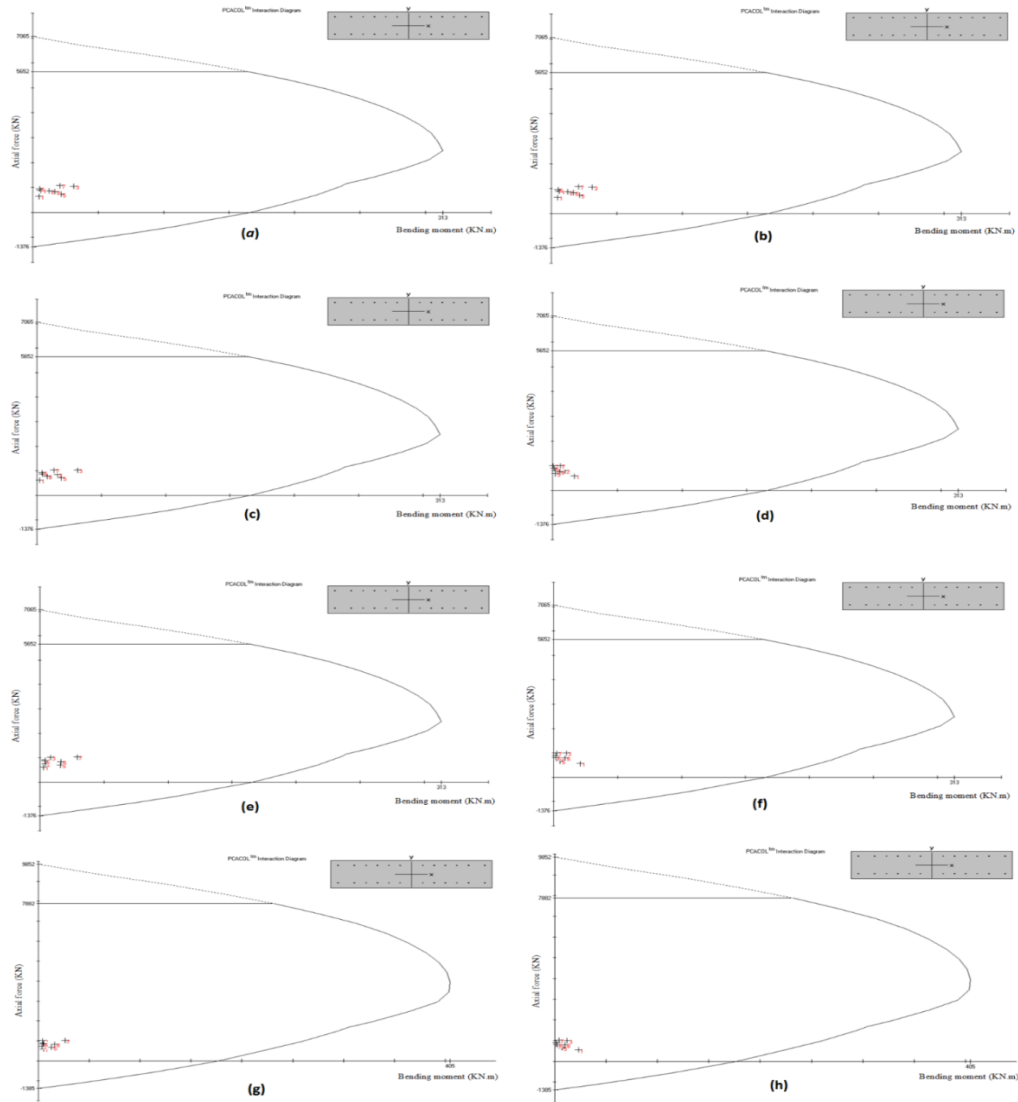
Consequently, using the PCA column, the stability of the twin-tube tunnels against the above-mentioned forces and moments is studied and the corresponding safety factors are assigned (Table 6).

The PCA column is a software program for designing and investigating the reinforced concrete sections subjected to the axial and flexural loads. In this software, after modeling the segmental lining with all specifications, the previously obtained forces and moments were exerted on the modeled profile. After evaluating the interaction between the axial and flexural loads and comparing it with the profile resistance, the PCA column estimates the safety factors corresponding to the exerted forces and moments [15].

In order to control the forces and moments exerted on the segmental linings of the twin-tube tunnels, the allowable stress design method was used. In the practice of tunnel engineering, it is normal to assume a factor of safety (FS = 1.5) for failure [16]. Figure 9 shows the axial-flexural load-interaction diagrams corresponding to the segmental linings of the Sahand and Sabalan tunnels in the different horizontal distances of the single-tube tunnel.

Table 6. Safety factors corresponding to the above-mentioned forces and moments.
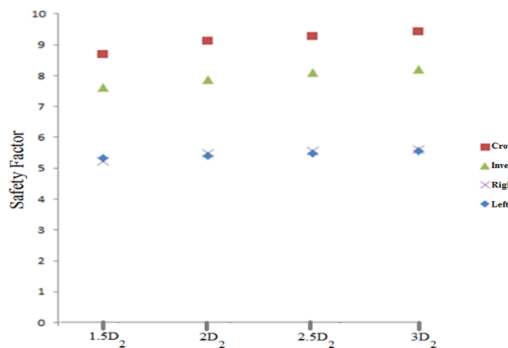
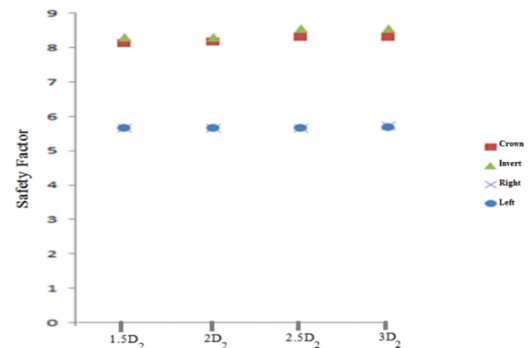| Tunnel's name	Check-point position	1.5D	2D	2.5D	3D
Sahand	Crown	8.68	9.11	9.26	9.42
	Up-right	6.72	7.24	7.43	7.56
	Right	5.23	5.48	5.54	6.07
	Down-right	5.88	6.05	6.17	6.23
	Down	7.62	7.88	8.09	8.19
	Down-left	6.32	6.45	6.52	6.63
	Left	5.32	5.41	5.48	5.55
	Up-left	6.46	6.59	6.72	6.83
Sabalan	Crown	7.17	8.17	8.29	8.29
	Up-right	7.43	7.43	7.85	7.89
	Right	5.65	5.65	5.65	5.72
	Down-right	6.14	6.28	6.28	6.28
	Down	8.31	8.31	8.56	8.56
	Down-left	6.89	6.89	6.89	6.89
	Left	5.65	5.65	5.65	5.69
	Up-left	7.06	7.06	7.06	7.06

Figure 9. Axial-flexural interaction diagrams for different horizontal distances. a) Sahand (L = 1.5D), b) Sabalan (L = 1.5D), c) Sahand (L = 2D), d) Sabalan (L = 2D), e) Sahand (L = 2.5D), f) Sabalan (L = 2.5D), g) Sahand (L = 3D), h) Sabalan (L = 3D)

The estimated safety factors corresponding to the points, located at the top, bottom, and on the sidewalls of the Sahand and Sabalan tunnels due to excavation of the single-tube tunnel are shown in Figures 10 and 11, respectively.

Figure 10. Estimated safety factors in the Sahand's segmental lining.

Figure 11. Estimated safety factors in the Sabalan's segmental lining.

In order to control the shear forces exerted on the segmental linings of the Sahand and Sabalan tunnels, Equation (1) was used.

$$V_n = V_c + V_s \tag{1}$$

where V_n is the shear resistance of the reinforced concrete profile, V_c is the shear resistance provided by the concrete, and V_s is the resistance provided by the longitudinal steel bars embedded in the segmental lining. In order to evaluate the shear resistance of the concrete and bended longitudinal bars, Equations (2) and (3) were used.

$$V_c = \frac{1}{6}\sqrt{f'_c}\,b_w d \tag{2}$$

$$V_S = 0.34 f_y A \tag{3}$$

In Equation (2), f'_c is the uniaxial compression of the concrete in MPa, and b_w and d are the width and thickness of the profile (in mm), respectively. In Equation (3), f_y and A are the yield stress of steel bars in MPa and the accumulated cross-section in mm^2, respectively. The cross-section of the segmental lining used in the twin-tube tunnels is shown in Figure 12.
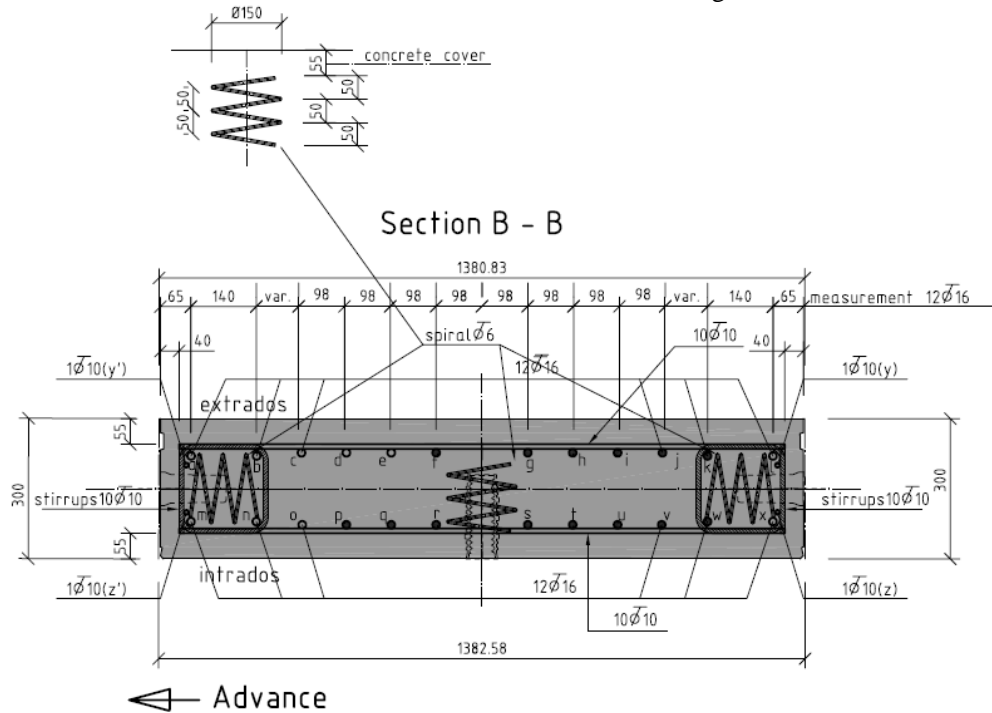

Figure 12. Cross-section of segmental linings of the twin-tube tunnels (distances are in mm).

As it can be seen, 24 steel bars (14 mm, AIII) with the accumulated cross-section of 3996 mm^2 were embedded in the section with the width and thicknesses of 1.4 m and 0.3 m, respectively. In order to evaluate the shear resistance using Equation (1):

$$V_c = \frac{1}{6} \times \sqrt{27.5} \times 1400 \times 300 = 367kN$$

$$V_s = 0.34 \times 392.4 \times 3696 = 493kN$$

$$V_n = 367 + 493 = 860kN$$

As it can be seen, decreasing the horizontal distance between the single- and twin-tube tunnels causes the exerted forces and moments to decrease. Consequently, the corresponding safety factors are increased. Considering the safety factor (1.5) for failure in urban tunneling, we can see that the segmental linings of the twin-tube tunnels have a high degree of stability against the exerted forces and moments. Also considering the shear forces exerted on the segmental linings of the twin-tube tunnels, it can be seen that the shear loads are well below the estimated shear resistance in all the horizontal distances.

4.3. Excavation stability of e single-tube tunnel

The basic concept of the design of the structures cannot be applied to the tunnels as stresses and strains are not reliably known. The critical strain is a better measure of failure. The critical strain (εc) is defined as a ratio between UCS and the modulus of deformation (Ed) of geo-materials [17]. The critical strain could be used successfully for assessing the displacement measurements in

tunnels such as crown settlements and convergence. Sakurai [17] has classified the hazard warning level into three stages in relation to the degree of stability. The relation of critical strain and Young's modulus was obtained by Sakurai, and he presented the hazard warning levels, as follows:

$$Log\ \varepsilon_c = -0.25 LogE - 0.85 \qquad (4)$$
Hazard warning level I

$$Log\ \varepsilon_c = -0.25 LogE - 1.22 \qquad (5)$$
Hazard warning level II

$$Log\ \varepsilon_c = -0.25 LogE - 1.59 \qquad (6)$$
Hazard warning level III

where E is the Young's modulus (Kg/cm^2). The hazard warning levels I and III indicate the long- and short-time stability of tunnel, respectively. The hazard warning level II is suggested as the base of tunnel design.

He observed that where strains in the roof ($\varepsilon_c = u_c/a$) were less than warning level I, there were no problems in the tunnels, whereas tunneling problems were encountered where strains approached warning level III. Regarding the value of Young's modulus (E) in the layer in which the

single- and twin-tube tunnels were laid (Table 1), the critical strain value for the hazard warning level II was calculated. This value is 0.013. The value of allowable displacement based on the hazard warning level II was determined using the values of critical strain and radius of the tunnel, as follows:

$$\varepsilon_c = \frac{u_c}{a} \qquad (7)$$

where u_c is the allowable displacement based on the hazard warning level II and α is the radius of the tunnel. By substituting the radius of the single-tube tunnel (4.75 m) and the critical strain (0.013), the allowable displacement on the section of the single-tube tunnel being excavated will be 0.061 m. By comparing the displacements obtained from the numerical models for different horizontal distances (Table 7), with the allowable displacement based on the hazard warning level II (0.061 m), it appears that the single-tube tunnel is stable in all distances.

The displacements occurring on the profile of the single-tube tunnel in the various horizontal distances are shown in Figure 13.
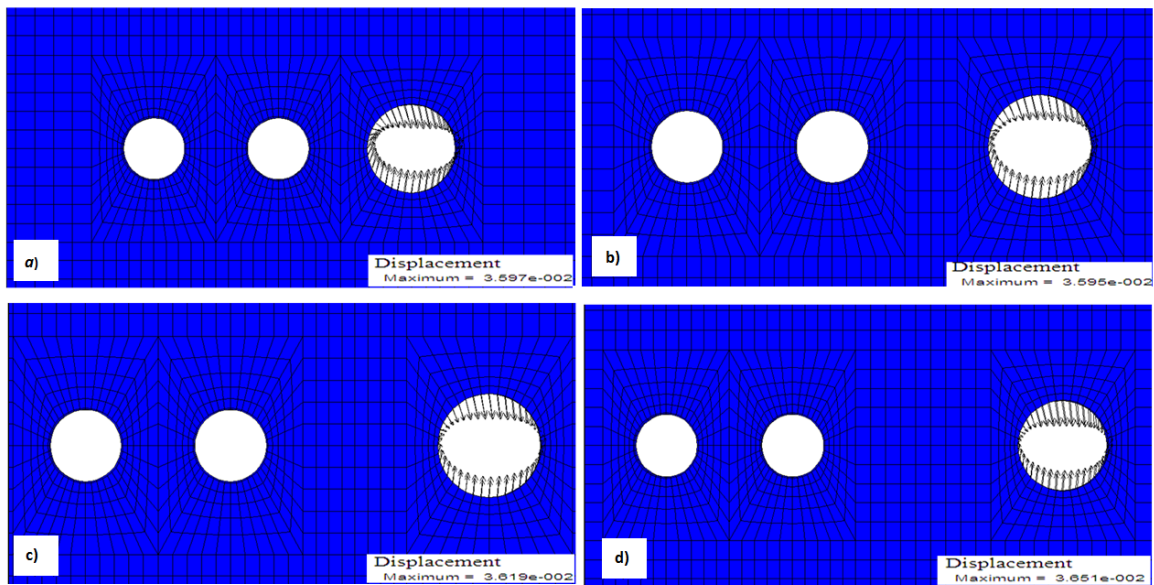

Figure 13. Displacements occurring on the profile of the single-tube tunnel being excavated. *a*) L = 1.5D₂, b) L = 2D₂, c) L = 2.5D₂, d) L = 3D₂

Table 7. Maximum displacements occurring on the profile of the excavating single-tube tunnel.

Horizontal distance between the single- and twin-tube tunnels (m)	Maximum displacement occurring on the profile of the single-tube tunnel (mm)
3D₂	36.51
2.5D₂	36.19
2D₂	35.95
1.5D₂	35.97

It can be seen that the single-tube tunnel is stable in all horizontal distances. As the horizontal distance decreases, the displacement vectors deviate toward the opposite side due to the effects of the existing twin-tube tunnels. No important relation was obtained between the displacement rate and the horizontal distances.

4.4. Surface subsidence

The damage classification proposed by Rankin [18] in 1988 (Table 8) applies to the frame buildings with isolated foundations or with pile foundations, where the distance among piles such that the "bearing group-effect" is not is triggered. The damage is related to the differential settlements among the isolated foundations, and the angular distortion β becomes the most relevant control parameter, which is also accompanied by the maximum settlement S_{max} (Figure 14).

In general, the threshold between category 2, aesthetic damages, category 3, and functional damages identifies two distinct families of causes. The damages related to category 2 or lower are the consequence of a combination of the causes related both to the intrinsic behavior of the building (plaster or concrete shrinkage, thermal variations, intrinsic elastic deformations, etc.) and the differential movements of the ground. Hence, this type of damage can be completely independent from the tunneling induced movements. On the other hand, the damages

related to a category higher than 2 are certainly related to the external causes. It should be pointed out that the above damage classifications are valid for buildings in good condition, i.e. without initial defects [19]. Figure 15 presents the vertical (z) displacement contours for the different horizontal distances between the single- and twin-tube tunnels. It can be seen that the magnitudes of the z-displacement are significantly affected by the horizontal distance between the tunnels. As expected, increasing the horizontal distance between the single- and twin-tube tunnels makes the z-displacement above the tunnels decrease.
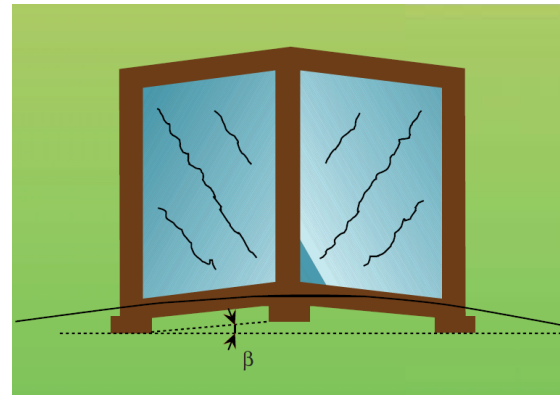

Figure 14. Probable behavior of framed buildings undergoing a "hogging mode" type of induced deformations.
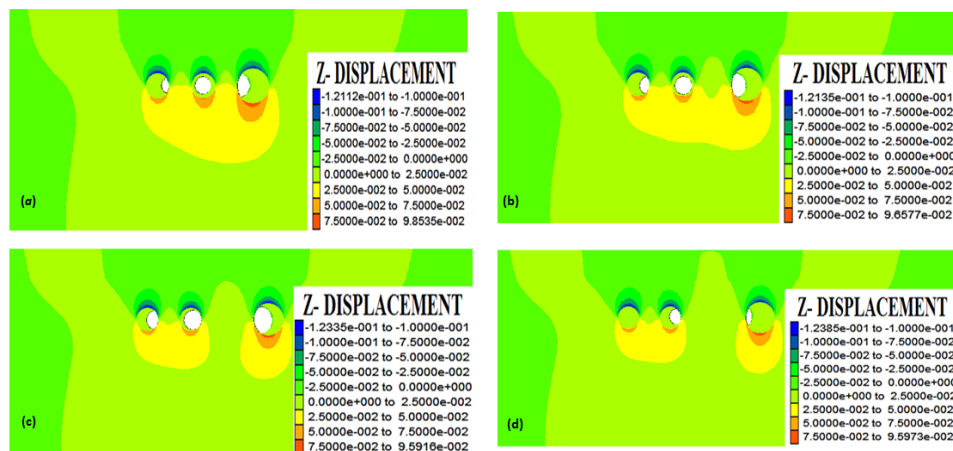

Figure 15. Vertical displacements for different horizontal distances. *a*) L = 1.5D$_2$, b) L = 2D$_2$, c) L = 2.5D$_2$, d) L = 3D$_2$

As shown in Figure 16, the horizontal distance between the proposed tunnels undoubtedly affects the surface settlement. This figure shows that the transversal settlement pattern in the surface after the tunnels is constructed. When the horizontal spacing is around 3D$_2$, the vertical displacements

between the single- and twin-tube tunnels are minimized. It can be seen that in the horizontal distance that equals 3D$_2$ (L = 3D$_2$), the single- and twin-tube tunnels behave separately on the surface settlement.

The results obtained show that the maximum surface settlement between the single- and twin-tube tunnels decreases when the horizontal distance increases. In the 1.5, 2, and $2.5D_2$ horizontal distances, the amount of the maximum settlement equals 15.25, 13.65, and 13.34 (in mm), respectively. The maximum surface settlement that occurs in the 1.5, 2, and $2.5D_2$ horizontal distances is shown in Figure 17.
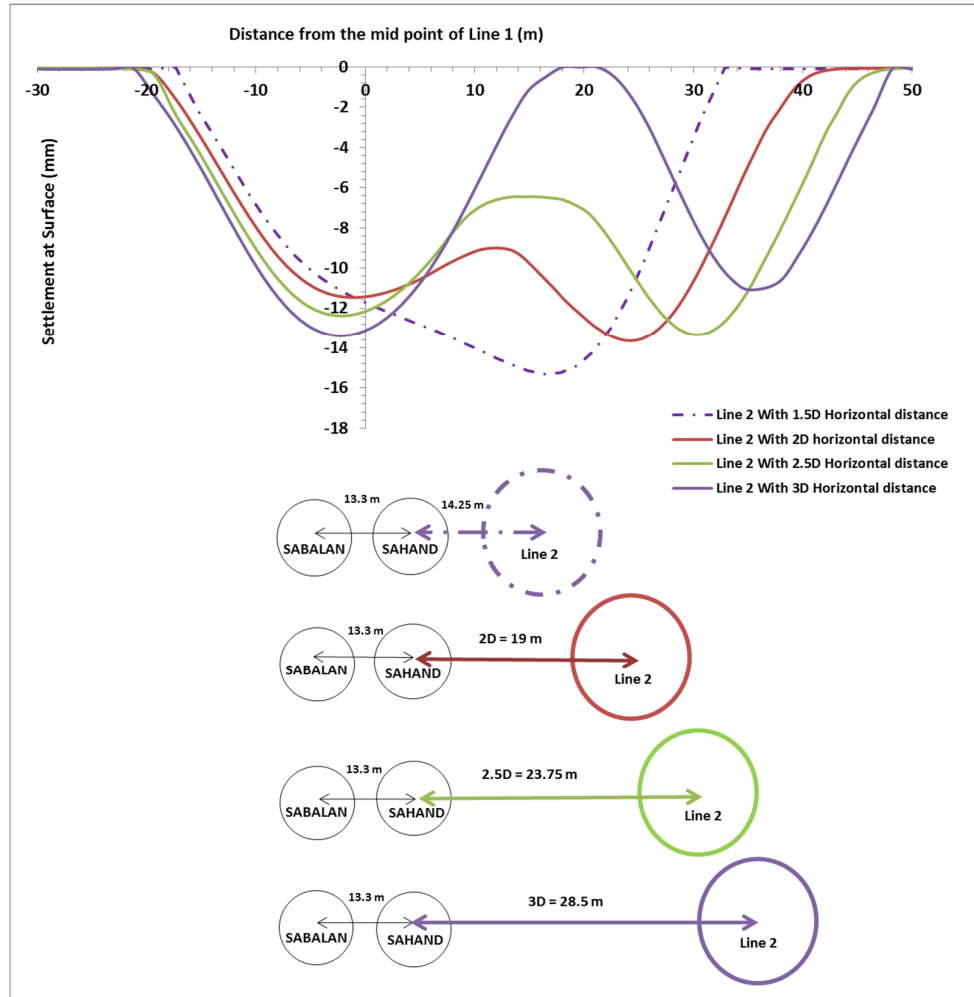

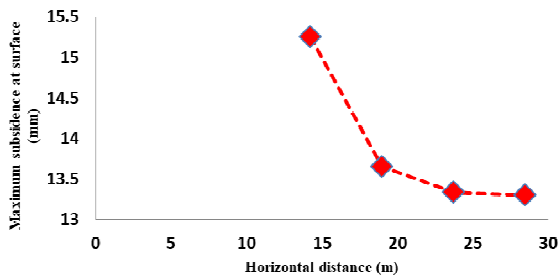**Figure 16. Surface settlement in different horizontal distances.**

Figure 17. Maximum surface settlement in different horizontal distances.

Considering the settlement diagrams related to the different horizontal distances, it can be seen that in the horizontal distance that equals $3D_2$, the maximum surface settlement occurs in the corresponding point of the mid-point of the twin-tube tunnels on the surface. When the horizontal distance decreases to 2.5, 2, and $1.5D_2$, the position of maximum surface settlement moves to the point corresponding to the single-tube tunnel's crown on the surface. The analysis also shows the maximum gradient of the surface settlement contour, and consequently, its influence on the surface structures changes with the horizontal distance in a way that for the horizontal distance equaling 1.5, 2 and $2.5D_2$, the maximum gradient of the settlement contour equals 1/750, 1/845, and 1/880, respectively. With reference to Table 8, it can be seen that in all the adopted distances, the estimated damage lies between the classes 1 and 2.
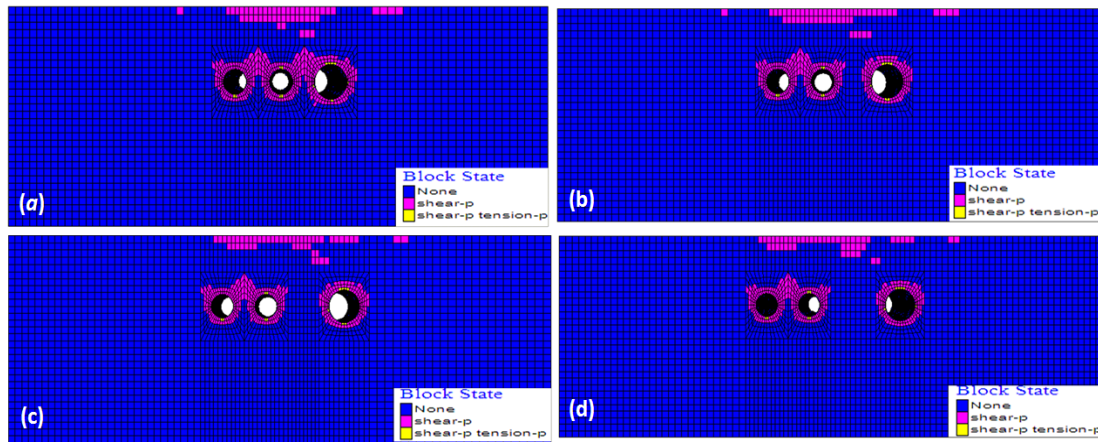
Table 8. Damage classification established by Rankin (1988).

Category of risk of damage	Degree of severity	Description of typical damage	Control parameters βmax Smax [mm]
1 Aesthetic	Negligible	Superficial damage unlikely	< 1/500 < 10
2 Aesthetic	Slight	Possible superficial damage that is unlikely to have a structural significance.	1/500–1/200 10–50
3 Functional	Moderate	Expected superficial damage to buildings and expected damage to rigid pipelines	1/200–1/50 50–75
4 Service-ability and structural	High	Expected structural damage to buildings and damage to rigid pipelines; possible damage to other pipelines	> 1/50 > 75

4.5. Pillar stability

One of the parameters that influence the interaction between the adjacent tunnels is the stability of the pillar lying between the tunnels.

Figure 18 presents the plasticized regions occurring between the twin- and single-tube tunnels with different horizontal distances of the single-tube tunnel.

Figure 18. Plasticized regions between the single- and twin-tube tunnels. *a*) L = 1.5D₂, b) L = 2D₂, c) L = 2.5D₂, d) L = 3D₂

It can be seen that in the horizontal distance that equals 1.5D₂, the plasticized regions include the whole pillar lying between the single-tube and Sahand tunnels. On the other hand, as it can be seen, the plasticized zones are in the shear-p condition, meaning that there could be some temporary instabilities during the excavation but the whole pillar is considered as stable [20]. In all of the above-mentioned criteria, the stability of the pillar lying between Sahand tunnel and the single-tube tunnel is the only parameter that strictly limits the horizontal distance and prevents distances less than 1.5D₂ from being chosen. Thus concerning the stability of the pillar lying between the Sahand tunnel and the single-tube tunnels, 1.5D₂ was chosen as the minimum allowable horizontal distance.

5. Conclusions

Underground structures are currently widely used, and are built as urbanism develops. Therefore, it is of prime importance to predict the possible interaction effects between the adjacent underground structures. In this work, considering various underlying criteria, the interactions between a large diameter single-tube tunnel being excavated close to the relatively small diameter twin-tube tunnels were investigated using a 3D numerical method. The following conclusions were made:

As the single-tube tunnel is being excavated close to the twin-tube tunnels, the cross-sections of the twin-tube tunnels move slightly to the opposite side and upward, depending on the horizontal distance of the single-tube tunnel.

The forces and moments exerted on the segmental linings of the twin-tube tunnels increase as the horizontal distance decreases. It can be inferred that in the distance that equals 3D₂, the effect of the excavation of the single-tube tunnel on the stability of the twin-tube tunnels is virtually negligible.

The maximum surface settlement decreases as the horizontal distance increases. When the horizontal distance is equal to $3D_2$, the excavation of the single-tube tunnel shows no significant effect on the twin tunnels. Also in this case, the hazard level in all distances lies between the categories I and II of the Rankin damage classification.

Considering the plasticized zones where the distance is equal to $1.5 D_2$, the plasticized zones include the whole column lying between the single-tube tunnel and the Sahand tunnel. With reference to the FLAC3D manual, the mentioned plasticized zones are not pulling an instability risk to the column and only happen periodically during the excavation. Choosing the horizontal distances less than $1.5D_2$ makes the column instable.

Finally, all the studied criteria approve the horizontal distance equal to $3D_2$ as the distance in which the interaction effects disappear.

References

[1]. Chakeri, H. and Ünver, B. (2014). A new equation for estimating the maximum surface settlement above tunnels excavated in soft ground. Environmental earth sciences. 71 (7): 3195-3210.

[2]. Soliman, E., Duddeck, H. and Ahrens, H. (1993). Two-and three-dimensional analysis of closely spaced double-tube tunnels. Tunnelling and Underground Space Technology. 8 (1): 13-18.

[3]. Kawata, T., Ohtsuka, M. and Kobayashi, M. (1993). Observational construction of large-scaled twin road tunnels with minimum interval. In Infrastructures souterraines de transports (pp. 241-248).

[4]. Perri, G. (1995). Analysis of the effects of the two new twin tunnels excavation very close to a big diameter tunnel of Caracas, subway. In International Journal of Rock Mechanics and Mining Sciences and Geomechanics Abstracts (Vol. 3, No. 32, p. 138A).

[5]. Yamaguchi, I., Yamazaki, I. and Kiritani, Y. (1998). Study of ground-tunnel interactions of four shield tunnels driven in close proximity, in relation to design and construction of parallel shield tunnels. Tunnelling and Underground Space Technology. 13 (3): 289-304.

[6]. Karakus, M., Ozsan, A. and Başarır, H. (2007). Finite element analysis for the twin metro tunnel constructed in Ankara Clay, Turkey. Bulletin of Engineering Geology and the Environment. 66 (1): 71-79.

[7]. Liu, H.Y., Small, J.C., Carter, J.P. and Williams, D.J. (2009). Effects of tunnelling on existing support systems of perpendicularly crossing tunnels. Computers and Geotechnics. 36 (5): 880-894.

[8]. Addenbrooke, T.I. and Potts, D.M. (2001). Twin tunnel interaction: surface and subsurface effects. International Journal of Geomechanics. 1 (2): 249-271.

[9]. Chehade, F.H. and Shahrour, I. (2008). Numerical analysis of the interaction between twin-tunnels: Influence of the relative position and construction procedure. Tunnelling and Underground Space Technology. 23 (2): 210-214.

[10]. Chakeri, H., Hasanpour, R., Hindistan, M.A. and Ünver, B. (2011). Analysis of interaction between tunnels in soft ground by 3D numerical modeling. Bulletin of Engineering Geology and the Environment. 70 (3): 439-448.

[11]. Sarfarazi, V., Haeri, H., Safavi, S., Marji, M.F. and Zhu, Z. (2019). Interaction between two neighboring tunnel using PFC2D. Structural Engineering and Mechanics. 71 (1): 77-87.

[12]. Abdollahi, M.S., Najafi, M., Bafghi, A.Y. and Marji, M.F. (2019). A 3D numerical model to determine suitable reinforcement strategies for passing TBM through a fault zone, a case study: Safaroud water transmission tunnel, Iran. Tunnelling and Underground Space Technology, 88, 186-199.

[13]. Mirsalari, S.E., Fatehi Marji, M., Gholamnejad, J. and Najafi, M. (2017). A boundary element/finite difference analysis of subsidence phenomenon due to underground structures. Journal of Mining and Environment. 8 (2): 237-253.

[14]. Lambrughi, A., Rodríguez, L.M. and Castellanza, R. (2012). Development and validation of a 3D numerical model for TBM–EPB mechanised excavations. Computers and Geotechnics, 40, 97-113.

[15]. Structurepoint (2012) spColumn Manual. Skokie, USA.

[16]. Carranza-Torres, C. and Diederichs, M. (2009). Mechanical analysis of circular liners with particular reference to composite supports. For example, liners consisting of shotcrete and steel sets. Tunnelling and Underground Space Technology. 24 (5): 506-532.

[17]. Sakurai S (1997) Lessons learned from field measurements in tunneling. Tunn Undergr Sp Tech 12 (4): 453-460. doi: 10.1016/S0886-7798(98)00004-2.

[18]. Rankin, W (1988) Ground Movements Resulting from Urban Tunnelling: Predictions and Effects. Geological Society London Engineering Geology Special Publications. 5 (1):79-92. doi: 10.1144/GSL.ENG.1988.005.01.06.

[19]. Guglielmetti, V., Grasso, P., Mahtab, A. and Xu, S. (Eds.). (2008). Mechanized tunnelling in urban areas: design methodology and construction control. CRC Press.

تحلیل تفاضل محدود سه بعدی تاثیر متقابل بین تونل بزرگ مقطع (منفرد) و تونل های دوقلو در محیط های شهری

صابر اکبری[1]، شکرالله زارع[1*]، حمید چاکری[2] و حسین میرزایی نصیرآباد[2]

1- دانشکده مهندسی معدن، نفت و ژئوفیزیک، دانشگاه صنعتی شاهرود، ایران

2- دانشکده مهندسی معدن، دانشگاه صنعتی سهند تبریز، ایران

* نویسنده مسئول مکاتبات: zare@shahroodut.ac.ir

چکیده:

ارزیابی تاثیر متقابل بین فضاهای زیرزمینی جدید و فضاهای موجود یکی از مسائل مهم در تونل سازی در محیطهای شهری میباشد. در ایـن تحقیـق، بـا اسـتفاده از نرم افزار FLAC3D، 4 مدل عددی از تونلهای منفرد و دوقلو در محیطهای شهری ساخته شده است که در آنها فاصله افقی بـین تونـل منفـرد و تونـلهـای دوقلـو تغییر میکند. هدف از این تحقیق بررسی تاثیرات تغییر فاصله افقی با در نظر گرفتن معیارهـای مختلـف از جملـه تغییرشـکل آسـتر (lining)، نیروهـا و ممـانهـای اعمال شده بر روی تونلهای دوقلو و فاکتورهای ایمنی آنها، نشست ایجاد شده در سطح زمین و ساختمانهای اطراف، پایـداری تونـل منفـرد و پایـداری سـتون قـرار گرفته بین تونلهای منفرد و دوقلو میباشد. با در نظر گرفتن معیارهای اشاره شده در بالا، نتایج بدست آمده نشان میدهد کـه تـاثیر متقابـل بـین تونلهـای منفـرد و دوقلو در فاصله افقی بیشتر از 3 برابر قطر تونل منفرد تقریبا ناچیز است. همچنین معیار پایداری ستون قرار گرفته مـابین تونلهـای منفـرد و دوقلـو از انتخـاب فاصـله افقی کمتر از 1/5 برابر قطر تونل منفرد جلوگیری میکند.

کلمات کلیدی: مدل سازی عددی سه بعدی، تاثیر متقابل بین تونلها، FLAC3D، تونل سازی در زمین های نرم.